Biogeosciences Discuss., 11, C6737–C6749, 2014
www.biogeosciences-discuss.net/11/C6737/2014/

Biogeosciences Discussions
Open Access

Interactive comment on "Tidal controls on trace gas dynamics in a seagrass meadow of the Ria Formosa lagoon (southern Portugal)" *by* E. Bahlmann et al.

E. Bahlmann

enno.bahlmann@zmaw.de

Received and published: 14 November 2014

Enno Bahlmann, Richard Seifert, University of Hamburg, Institute for Biogeochemistry and Marine Chemistry, Bundesstraße 55, 20146 Hamburg, Germany

The main concern of the reviewer is that the chamber design may lead to biased fluxes. Here we provide a more extensive description of the chamber system and show atmospheric data obtained during the campaign supporting the flux dynamics observed with our chamber. We would like to point out that the main focus of this manuscript are i.) to show the strong imprint of the tides on trace gas fluxes in coastal ecosystems and ii.) to highlight the importance of accurately addressing the perturbations of turbulent

Full Screen / Esc
Printer-friendly Version
Interactive Discussion
Discussion Paper

flows in flux chamber studies. Both points may have severe implications for our understanding of trace gas dynamics in coastal ecosystems. Regarding the magnitude of the fluxes during submersion we agree with the reviewer and have clearly stated this in the manuscript on page 10587, line 9-12: “As the strength of advection in our chamber system relative to ambient conditions is unknown we can currently not appraise the quality and reliability of the difference chamber systems “.

Atmospheric mixing ratios of CO2 and CH4

In particular during periods of low wind speeds and during easterly winds the atmospheric mixing ratios of CH4 and CO2 support the observed tidal imprint on the trace gas fluxes (fig. 1 and 2). Throughout the campaign the atmospheric mixing ratios of CO2 (average from both heights) ranged from 395.5 to 429.7 ppm (both heights) and averaged 400.3 ppm. The atmospheric mixing ratios of CH4 ranged from 1.831 to 1.895 ppm (both heights) and averaged 1.861 ppm. Lowest mixing ratios of 395.8$\pm$0.2 ppm for CO2 and of 1.834$\pm$0.004 ppm for CH4 were observed between 8:00 pm on April 25th and 4:00 am on April 26th and coincided with westerly winds from the Open Ocean and wind speeds above 4m/s. With decreasing wind speeds and during easterly winds, when the air masses passed over large parts of the lagoon the atmospheric mixing ratios of CO2 and CH4 increased. The close coupling between the measured fluxes and the atmospheric mixing ratios at low wind speeds becomes in particular evident at the end of the campaign. Over the last two tidal cycles the atmospheric mixing ratios of CH4 nicely resemble the enhanced emissions during immersion. The sharp methane emission peak observed when the water entered the chamber becomes diffuse under ambient conditions as bubble ebullition will occur throughout rising tide. On April 27th this coupling is somewhat confounded because of rapidly changing wind conditions. Nevertheless, elevated CH4 mixing ratios coincide with elevated fluxes during tidal immersion. As for CH4 elevated mixing ratios of atmospheric CO2 coincide with periods of strong CO2 emissions during tidal immersion at night. Notably on April 26th at noon the atmospheric CO2 mixing ratios show a slight drop when carbon assimila-

BGD

11, C6737–C6749, 2014

tion was largest. In conclusion the pattern of the atmospheric mixing ratios support the flux pattern observed with the chamber.

Operation Principle of the flux chamber

A During air exposure During air exposure the chamber operates as a conventional dynamic flux chamber (DFC). Briefly, the surface of interest is enclosed with a chamber and air is drawn through the chamber at a predefined flow rate. Net fluxes above the covered surface are calculated from the concentration difference between the inlet and outlet of the chamber assuming steady state conditions:

F_net=Q_n/A (c_out-c_in) (1)

where FNet is the net flux [M L-2 t-1], QN is the flushing flow rate through the chamber [L^3 t-1, at 1013.25 mbar and 298.15 K], cout and cin are the concentration of target compounds [M L-3] at the outlet and the inlet of the flux chamber and A is the bottom surface area of the flux chamber [L2]. M, L, and t are dimensions of mass, length, and time, respectively. A basic assumption of DFC-measurements is that the chamber is in steady state meaning that the time averaged net flux calculated from the inlet and outlet concentrations equals the time averaged net flux across the interface of interest. A convenient measure for the time required to establish steady state conditions is the response time (tr) of the chamber denoting the time after disturbance (such as a sudden change in emission) required to achieve 37% (e-1x 100) of the initial perturbation. Provided that the change after a perturbation is exponential 95% of steady state will be reached after three times the response time. Under aerial conditions the response time can be estimated from the flushing flow rate and the chamber volume and is given by

t_r = V/Q (2)

At a typical flushing flow rate of 3 L min-1 the response time of our chamber system is 2 minutes. Pre-tests revealed that complete mixing of the chamber volume is achieved

BGD

11, C6737–C6749, 2014

within 0.4 min. Hence with respect to our sampling frequency we can safely assume complete mixing of the air inside the chamber.

The physical nature of trace gas fluxes across natural interfaces is commonly described in terms of multiresistance models Gao et al., 1997; Zhang et al., 2002):

F_i=(c_s-c_ag)×h_i=(c_s-c_a)/R_i (3)

Where Fi denotes the flux across the interface, cs is the concentration in the sediment, cg is the gas concentration on the air side of the interface hi [L t-1] is the overall exchange coefficient and Ri [t L-1], the reciprocal of hi, is the overall transport resistance. The overall transfer resistance is given by the sum of the transfer resistance of the quasi laminar boundary layer above the sediment (Ra) and the diffusive resistance of the sediment surface layer (Rs)

R_i=R_a+R_s (4)

Ra is dependent on the aerodynamic properties of the chamber whereas Rs is dependent on the sediment properties. The sensitivity of the overall flux against the aerodynamic properties depends on the magnitude Ra and Rs. When both share the same magnitude the flux across the interface depends on Ra and Rs. On the other hand, when Rs becomes large relative to Ra the flux is governed by Rs and not affected by the aerodynamic properties of the chamber. In order to determine Ra for our flux chamber we have determined the CO2 flux above 1N NaOH. 4 L of 1N NaOH were carefully filled into a 10L Duran glass bottle avoiding wetting of the bottle walls and leaving a headspace of 6L being comparable to the headspace of the field chamber. The NaOH solution was gently stirred (50 RPM). Ambient air (407±3 ppm CO2) was pumped through the chamber at flushing flow rates between 0.5 and 5 L min-1 and the concentration was measured at the outlet of the chamber. Under the assumption that the NaOH solution provides a perfect sink for CO2 Rs becomes negligible and Ra can be estimated according to:

BGD

11, C6737–C6749, 2014

R_a= ãĂŰ-cãĂŮ_out/(c_out-c_in)×A/Q (5)

From 0.5 to 4 Lmin-1 the uptake flux increased logarithmically from 16.4 to 57.4 mmol m^2h-1 (F = 19.224*ln(Q) + 29.697; R2 = 0.9967) and remained on this level with a further increased flushing flow rate of 5 L min-1. Surprisingly Ra increased with increasing flushing flowrate from 0.162 hm-1 (Q= 0.5 L min-1) to 0.206 h m-1 at Q = 5.0 L min-1. We attribute this increase to an insufficient renewal of the liquid surface film limiting the CO2 uptake at high CO2 loads. However, these results provide an upper estimate of 0.162 hm-1 for Ra. The sediment side transfer resistance is commonly computed from the diffusivity of the sediment surface layer and its thickness (Gao et al., 1997; Zhang et al., 2002).

R_s=l/(0.6D_0 p_s) (6)

Where l [L] denotes the thickness of the sediment surface layer, 0.6 is an empirical scaling factor accounting for the tortuosity of the pores (Penman 1940 a,b), D0 [L2 t-1] is the diffusion coefficient in air and ps is the fraction of the air filled pore space. Following Zhang et al. (2002) we used a thickness of 0.005 m to estimate Rs. With D0(CO2) = 0.054 m^2 h-1 and ps ranging from 0.01 to 0.1 for water logged intertidal sediments Rs is estimated to range from 1.54 to 15.4 h m-1 being about one to two orders of magnitude larger than Ra. Given this it is reasonable to assume that the trace gas flux across the sediment surface is mainly governed by the sediment resistance. Further our tests suggest a minor effect of the flushing flow rate on the atmospheric transfer resistance making the overall transfer resistance insensitive against the aerodynamic properties of the chamber. The same principles apply to the trace gas exchange across the sea grass leafs. In contrast to higher plants on land seagrass lacks any stomata and gas transport is facilitated across the thin cuticle of the seagrass. MacFarlane (1992) reports a CO2 permeability of 2.1 μm s-1 for the cuticula of submersed plants. This corresponds to a transfer resistance of 132 h m-1. Using a leaf area index of 3 - 5 for Z. noltii in the Ria Formosa (Pérez-Lloréns & Niell, 1993) we can normalize the transfer resistance to the enclosed surface area and estimate its range to 26.5 to 46

Full Screen / Esc
Printer-friendly Version
Interactive Discussion
Discussion Paper

h m-1. In summary we can safely assume that during air exposure the gas exchange across the sediment surface and the seagrass leafs is not dependent on the aerodynamic properties of the chamber. The measured trace gas fluxes may be affected by the enclosure effect (i.e. the deviation of the internal trace gas concentration from ambient concentrations above the ground). The effect of the flushing flow rate depends on the overall transfer resistance. When assuming a constant and uniform source (or sink) the effect of the flushing flow rate under steady state conditions is given by (eq. 22. in Zhang et al., 2002):

F_steady=(c_s-c_i)/R_i $\times$1/(1+A/(R_i$\times$Q)) (7)

Thus the enclosure effect is given by:

F_steady/F_(limQ$\rightarrow\infty$) =1/(1+A/(R_i$\times$Q)) (8)

With a bottom surface area of 0.037 m^2 and an overall transfer resistance ranging from 1.62 to 15.6 h m-1 the steady state flux at a flushing flow rate of 3 L min-1 [0.18 m^3 h-1) resembles more than 96% of the maximum flux (F_(limQ$\rightarrow\infty$)) suggesting a negligible effect of the flushing flow rate. B During submersion Under submerged conditions we have to consider an additional transfer resistance for the air water transfer of the dissolved trace gases. Thus we will start our discussion with this additional transfer resistance. The dissolved trace gas is stripped out and the flux will depend on its volatility (given by the inverse Henrys law constant) and the water air transfer resistance of the chamber system. In analogy to the air sea gas exchange the flux of a trace gas can be computed as:

F=k_ch$\times$(c_w$\times$H_inv-c_g)=((c_w$\times$H_inv-c_g))/R_ch (9)

where kch is the gas exchange velocity [L t-1] depending on the flushing flow rate (Q) and the chamber design (in particular the chamber geometry and the gas bubble geometry), Rch = 1/kch is the corresponding transfer resistance, cw is the water concentration [m L-3], cg is the concentration in the gas phase inside the chamber, and

Full Screen / Esc
Printer-friendly Version
Interactive Discussion
Discussion Paper

Hinv is the inverse dimensionsless Henry's law constant. Under steady state conditions cg equals cout and F equals Fnet. Combination of eq. 9 with eq.1 leads to:

((c_w×H_inv-c_out))/R_ch =(c_out-c_in)Q/A (10)

and rearrangement leads to:

R_ch= ((c_w×H_inv-c_out)×A)/((c_out-c_in)×Q) (11)

Rch was determined in a similar manner as Ra. To mimic submersed conditions the chamber was filled with 1N NaOH Then ambient air was pumped through the chamber with flushing flow rates ranging from 0.5 to 6 L/Min. Due to the rapid transformation of dissolved CO2 to bicarbonate, cw x Hinv is assumed to become negligible. Thus Rch can be computed from eq. 5. R_ch= (ãĂŰ-cãĂŮ_out×A)/((c_out-c_in)×Q) (5)

Rch averaged 0.031±0.006 h m-1 and showed a slight decrease with increasing flushing flow rate that may be attributed to the purge gas dispersion inside the chamber. During submersion the interfacial resistance for diffusive transport across the sediment/water and water/leaf interface will be larger than during air exposure (1.54 to 15.4 h m-1 and 26.5 to 46 h m-1) because of the lower diffusivity of trace gases in water. Thus as for aerial conditions we can assume that diffusive fluxes are primarily governed by the interfacial resistance while the transfer resistance of the chamber Rch has a minor influence on diffusive trace gas fluxes. Our field data clearly show that during submersion the sediment/water flux is governed by advective transport. A treatment of these processes is beyond the scope of this paper as it would require detailed hydrodynamic data of the chamber system. On the other hand the fluxes across the water leaf interface are clearly governed by diffusion. Thus we limit the following discussion to diffusive exchange processes. Under submersed conditions the response time of the chamber will apparently depend on the solubility of the trace gases and in case of CO2 also on the carbonate system. The response time of the submersed chamber was derived from the slope of concentration over time at the outlet of the chamber after injection of seawater enriched in methane and CO2 respectively. For these tests arti-

Full Screen / Esc
Printer-friendly Version
Interactive Discussion
Discussion Paper

ficial seawater with 35 PSU was prepared from commercially available sea salt. Prior to the experiments the pH was adjusted to 8.1±0.1. DIC was adjusted to yield an atmospheric equilibrium concentration of 350±20 ppm. The chamber was continuously purged either with synthetic air (Westfalen, Germany) or synthetic air doped with CO2 (Westfalen Germany) providing a pCO2 of 350±20 ppm in the purge gas. The purge flow was set to 3.0 L min-1. 50 ml of seawater were withdrawn from the chamber and were equilibrated with either methane (30% in synthetic air) or CO2 (30% in synthetic air) for 24h at 1.3 bar and 4°C. These solutions were injected into the chamber and the decline in pCH4 and pCO2 was measured over time. A second set of experiments was carried out to monitor the CO2 uptake. Prior to these experiments the chamber was flushed with pure synthetic air for several hours to lower the DIC inside the chamber. During the CO2 measurements the pH inside the chamber was measured with a Schott CG 841 pH meter. The evolution of the CO2 outlet concentration and the CO2 flux is exemplified for CO2 uptake in figure 3. Complete mixing of the water inside the chamber as indicated by the pH was achieved within 1.10 minutes. The response time of the chamber towards changes in the pCH4 was 1.20± 0.20 min and the response time of the chamber towards changes in the DIC system was dependent on the pH, reflecting the residence time of CO2 in water with respect to hydration and reaction with OH-, and ranged from 49 to 67 min. with pH ranging from 7.80 to 8.40. Thus we can estimate the time for re-establishing a steady state to 3.60±1.0 min. for CH4 and to about 170±30 min. for DIC. When assuming a constant source / sink inside the chamber and a response time of 60 min., 37% of the source / sink will be replenished after 1h and 80% after 6h of incubation. Thus our dynamic chamber can in principal capture changes in the DIC pool over longer incubations times but will smooth the initial signal. During tidal inundation the chamber is connected to the surrounding waters via U-tube at the bottom (stainless steel tube 50 cm length, 4 mm i.d.) to assure pressure equilibrium. This inevitably leads to an exchange of water between the chamber and the surrounding water body that may thus affect the flux measurements. The flux through the U-tube depends on the pressure gradient between the chamber and the surrounding water

BGD
11, C6737–C6749, 2014

and is thus mainly modulated by wave actions. The flux measurements were carried out under calm conditions with wind speeds rarely exceeding 5 ms-1 and wave heights below 10cm. For a pressure difference of 1 kPa is the measured flow was 308±7 ml min-1. This is about 46% of the theoretical flow expected from Hagen-Poiseilles law reflecting the narrowing of the tube at the bendings. The wave induced pressure oscillations cause an oscillating flow between the chamber and the surrounding water body. For sinusoidal waves with an amplitude of 5cm the water exchange rate is 46 ml min-1 resulting in a response time towards water exchange of 2.15h being substantially larger than the respective response times for the gas exchange. For CH4 we can safely assume that the bias due to water exchange is less than 1%, regardless of the concentration difference between the chamber and the surrounding water. For CO2 the bias only is less than 3%. Due to the much slower response of the carbonate system the bias with respect to DIC may become substantially larger. From the respective response times we can estimate an upper limit for the bias of 32±3% e.g. when the chamber exchanges with DIC free water. Benthic respiration and assimilation will shift both DIC pools into the same direction. Due to the enclosure effect the shift is more pronounced inside the chamber. In typical coastal waters (Alkalinity = 2200 μeq, pH (8.185, DIC = 1999 μmol, pCO2 = 380 ppm) a change of 1% in the DIC changes the pCO2 by about 10%. As a consequence, gas exchange is more sensitive to changes in DIC then the water exchange. For a difference in the DIC concentrations of 20% we have carefully estimated the bias to be in the range of 12 to 18%. We found this acceptable for a first tentative assessment of the DIC dynamics over full tidal cycles as was the primary goal of our study.

References Gao, F., Yates, S.R., Yates, M.V., Gan, J.Y., Ernst, F.F., 1997. Design, fabrication, and application of a dynamic chamber for measuring gas emissions from soil. Environmental Science & Technology 31, 148-153. Penman, H.L. 1940a. Gas and vapor movements in the soil. I. The diffusion of vapors through porous solids, J. Agr. Sci., 30:437–462. Penman, H.L. 1940b. Gas and vapor movements in the soil. II. The diffusion of carbon dioxide through porous solids, J. Agr. Sci., 30:570–581.

MacFarlane J.J 1992 Perm Permeability of the cuticle of Vallisneria spiralis to carbon dioxide and oxygen, Aquatic Botany 43: 129-135 Pérez-Lloréns JL, Niell FX (1993) Seasonal dynamics of biomass and nutrient content in the intertidal seagrass Zostera noltii Hornem. from the Palmones river estuary, Spain. Aquat Bot 46:49–66 Zhang, H., Lindberg, S.E., Barnett, M.O., Vette, A.F., Gustin, M.S., 2002. Dynamic flux chamber measurement of gaseous mercury emission fluxes over soils. Part 1: simulation of gaseous mercury emissions from soils using a two-resistance exchange interface model. Atmospheric Environment 36, 835-846.

Please also note the supplement to this comment:
http://www.biogeosciences-discuss.net/11/C6737/2014/bgd-11-C6737-2014-supplement.pdf

---

Interactive comment on Biogeosciences Discuss., 11, 10571, 2014.

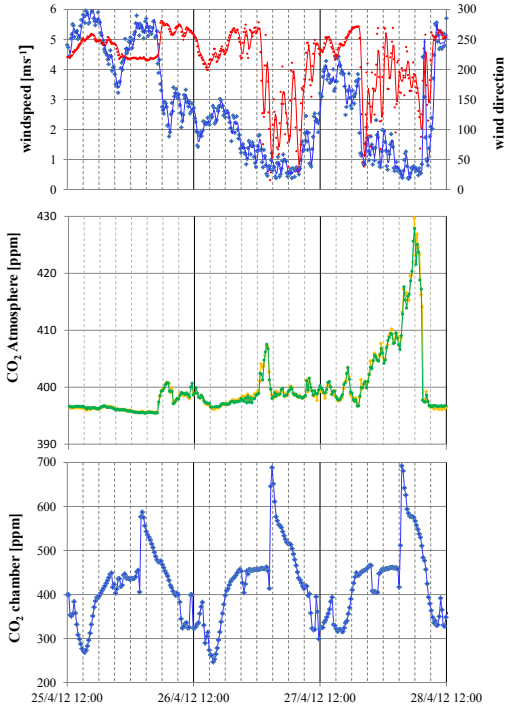

Fig. 1. Time series of CO2 mixing ratios at the chamber outlet, in the atmosphere and meteorological conditions, upper panel wind direction in red 60 min moving average, wind speed in blue 60 min moving avera

BGD
11, C6737–C6749, 2014

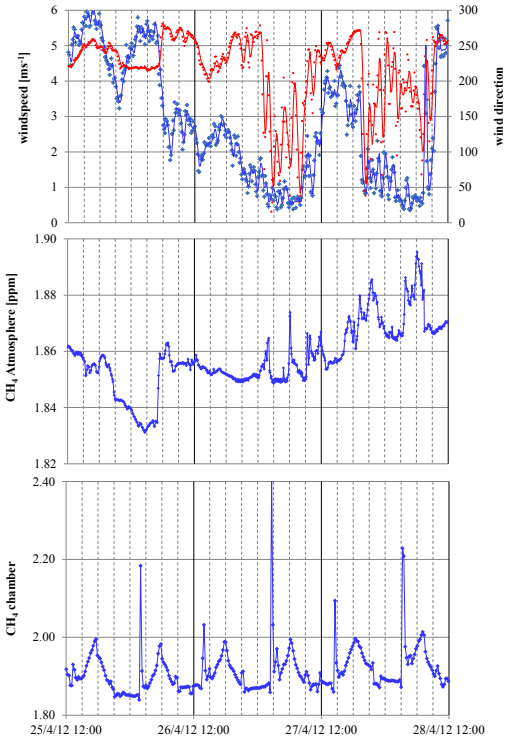

Fig. 2. Time series of CH4 mixing ratios at the chamber outlet and in the atmosphere along with meteorological conditions, upper panel wind direction in red 60 min moving average, wind speed in blue 60 min mo

Full Screen / Esc
Printer-friendly Version
Interactive Discussion
Discussion Paper

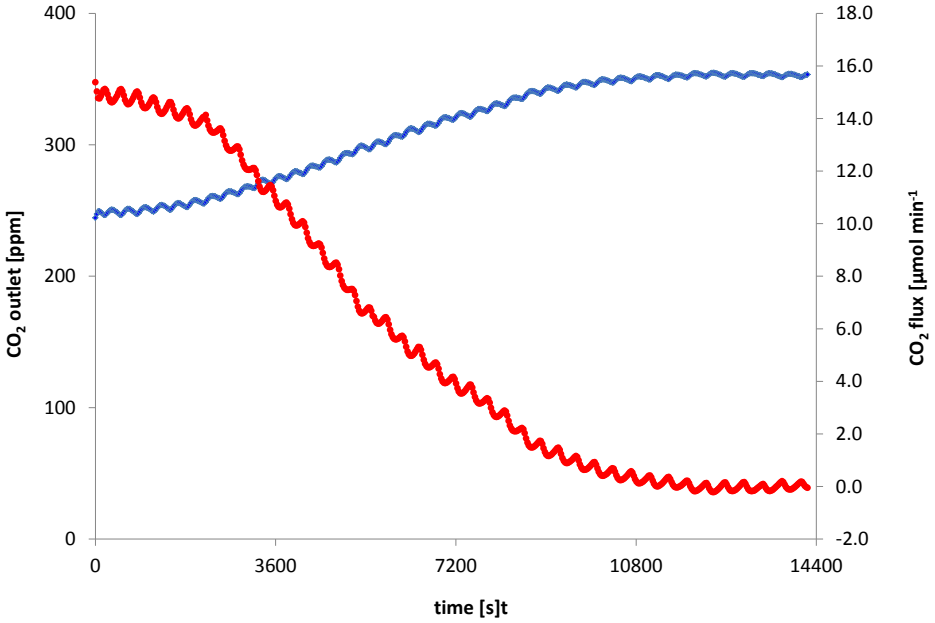

Fig. 3. Figure 3: Evaluation of the response time of the chamber system. The Co2 outlet concentration on the left axis is shown in blue, the CO2 flux is shown in red. Steady state is reached after 11800s. The

BGD
11, C6737–C6749, 2014